



# Numerical Evaluation of 2D Versus 3D Simulations for Seismic Slope Stability

Fernando Della Pasqua, Rafael Benites, Chris Massey, and Mauri MacSaveney

## Abstract

Seismic slope stability hazards assessments based on two-dimensional (2D) analyses limits the interpretation to in-plane motion. This means that the effects on ground motions due to lateral heterogeneity contributed by internal wave reflection are neglected. In this study we assess to which extent a 2D model of a simple topographic crest (spur) is valid, using equivalent 3D simulations. The study shows that seismic analysis based on the analysis of 2D cross sections of slopes with irregular topography such as spur crest lines can misrepresent the response of the slope at the surface. Regular slope geometries representing a laterally infinite slope can be well represented by 2D analyses, however as the slope becomes laterally irregular, the topographic contribution needs to be given careful consideration by way of 3D simulations.

## Keywords

Seismic • Amplification • Slope stability

## Introduction

Seismic slope stability hazards assessments carried out using numerical simulation of ground motion based on two dimensional (2D) cross-sections, of the three dimensional (3D) “real” topography of the slope, are limited by the effect of lateral heterogeneity on ground motions resulting from lateral internal wave scattering. These limitations were highlighted in recent seismic slope hazard assessments carried out at the Port Hills which involved 2-dimensional analysis only using Quake/W (e.g., Massey et al. 2014). As a follow up, in this study we assess the validity of the 2D

simulation of ground motion for seismic slope stability hazard of irregular 3D topographies.

## Methodology

First we verify wave propagation outputs of two software programs generally used for dynamic slope stability assessments, namely Quake/W (Slope/W 2012), FLAC3D (Itasca 2005) and Boundary Integral (Wong and Jennings 1975; Zeng and Benites 1998); against the analytical solution for a 2D half-space using a vertically incident pulse. This verification was carried out by comparing the response of numerical simulations of 2- and 3-dimensional grid models, with the 3D slope geometry represented by smooth (laterally infinite) and irregular (spur) slope topographies.

## Slope Geometry

The topographic profile used for the numerical analysis is based on a previously studied 70 m slope of the Port Hills at

F.D. Pasqua (✉) · R. Benites · C. Massey · M. MacSaveney  
GNS Science, PO Box 30368, Lower Hutt, 5004, New Zealand  
e-mail: f.dellapasqua@gns.cri.nz

R. Benites  
e-mail: r.benites@gns.cri.nz

C. Massey  
e-mail: c.massey@gns.cri.nz

M. MacSaveney  
e-mail: M.MacSaveney@gns.cri.nz

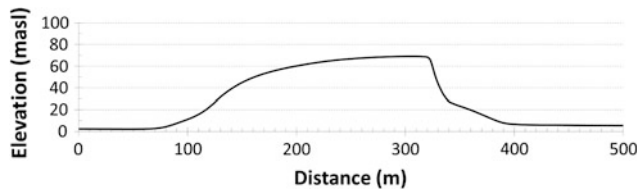


**Fig. 1** Topographic profile used in 2-dimensional analysis. After Cross section no. 2 of Massey et al. (2014). ST1 (10 m behind crest) and ST2 (100 m in front of crest) show location of recording stations

Richmond Hill (Cross section no 2 of Massey et al. 2014). The cross section profile used for the assessment is shown in Fig. 1.

The effect of 3D topographic variation was assessed by comparing a “regular” slope and an “irregular” slope crest. The regular slope grid was generated by extending the 2D profile (Fig. 1) laterally along strike 100 m either side. A graphic representation of the regular slope grid mesh used to carry out the 3D simulations is shown in Fig. 2. The irregular slope crest was generated with an apex angle of approximately 100 degrees based on spur slopes previously studied at the Defender Lane site, port Hills (Della Pasqua et al. 2014). A graphic representation of the regular slope grid mesh used to carry out the 3D simulations is shown in Fig. 2. The grid mesh size used varied from 3 to 4 m.

## Material Properties

A homogeneous medium was used with material properties based on those derived for volcanic breccias of the Richmond Hill slope (Massey et al. 2014). The value of input material properties used in the simulations are shown in Table 1. Linear elastic deformation was adopted and no mechanical damping was applied to the simulations to allow direct comparison of the topographic effects without imposing attenuation on the first peak arrivals.

## Input Motion

On applying the software programs to a geological structure of interest, the maximum frequency value for wave propagation must be defined to determine the minimum grid size capable to compute the propagation of waves. This maximum frequency can be determined from the input time series and can also be prescribed by taking into account wavelength dimensions comparable to the smallest geological heterogeneity of interest. The input motion used for the assessment was a Ricker wavelet (Ricker 1977) of peak frequency 7 Hz and peak amplitude of 0.5 m/s (Fig. 3). This pulse was applied at the base of all models.

## Output Parameters

The outputs used for comparison were the horizontal surface velocity and horizontal surface acceleration. The amplification effects were calculated as the maximum value relative to the base of the slope (e.g., Crest/Toe ratio) and relative to the input motion (e.g., Crest/Input ratio). Crest responses were recorded at a station 10 m away from the slope edge. Stations were also positioned at 5 m spacing along a 60 m line away from the crest.

## Evaluation of Slope Crest Amplification

To evaluate topographic effect a two stage comparisons was carried out using FLAC-3D in two stages. Stage 1: Comparison between 2D and 3D for a regular slope geometry. This involved crosschecking the results obtained from the 2D cross section (e.g., Fig. 1) to those obtained by carrying out the analysis using a 3D mesh (e.g., Fig. 2). Stage 2: Comparison between 3D response for a regular slope geometry (e.g., Fig. 2) and an irregular slope (spur) (e.g., Fig. 2).

**Fig. 2** Mesh used to represent 3-dimensional regular (left) and irregular (right) crest morphology

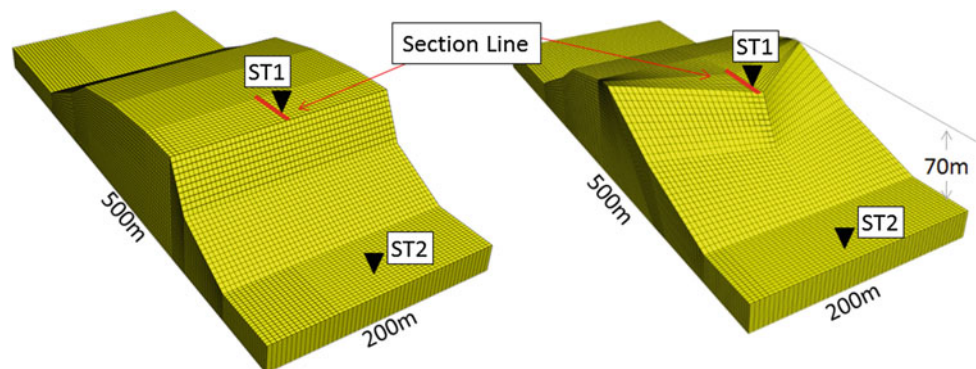


**Table 1** Material properties used for input parameters

Property	Value
Shear wave velocity ( $V_s$ )	800 m/s
Shear modulus (Gs)	$1.3 \times 10^9$ Pa
Density ( $\rho$ )	2000 kg/m <sup>3</sup>
Poisson ratio ( $\nu$ )	0.3
Damping ratio	0

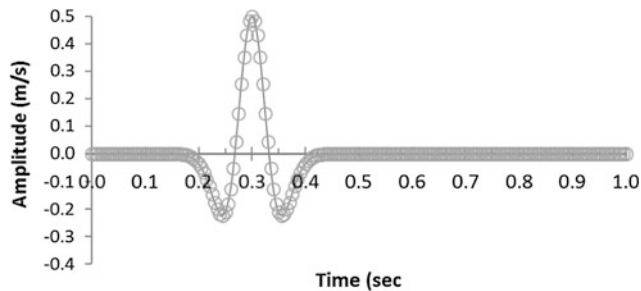


**Fig. 3** Ricker wavelet used as input motion for numerical analysis. Peak frequency = 7 Hz, Amplitude = 0.5 m/s

### Method Verification

Verification of the software numerical outputs was first carried out by performing generic Half-Space Tests. In these tests the response of a single vertically travelling cosine pulse was simulated in a rectangular elastic medium, and comparing the results to analytical solutions. Five tests were applied, which allowed both the results and software to be verified:

- Test 1: Amplitude during propagation
- Test 2: Arrival time
- Test 3: Amplitude at the surface
- Test 4: Amplitude after reflection, and
- Test 5: Polarity after reflection.

A diagram illustrating this set up for these numerical tests is shown in Fig. 4.

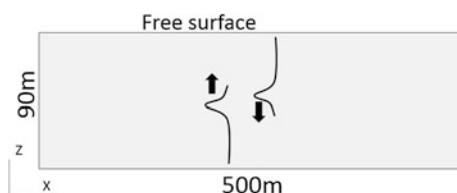


**Fig. 4** Flat-surfaced model used to represent a half-space and used to verify numerical response. Pulse initiates at the base and propagates vertically through an elastic medium

## Results

### Verification Test 1: Amplitude of the Propagating Wave

A pulse applied as a plane wave along the base of the elastic grid shown in Fig. 4 should experience no attenuation during travel. This means that the amplitude of the simulated pulse as it travels through the elastic medium should have the same amplitude as the input pulse. Figure 5 shows results for the amplitude of peaks simulated after 10 and 55 m travel distance. The input peak and calculated reflected peaks at 10 and 55 m above the base, as well as the peak at the surface are shown in Fig. 5a. The simulations obtained using F3D are shown in Fig. 5b and match the expected pulse shown in Fig. 5a. The Quake/W simulations (Fig. 5c) also match the calculated response however Quake/W continues to generate pulse reflections at the base causing, peak signals to continue after 0.5 s as shown in Fig. 5c. This is clearly illustrated by the peaks at 0.59, 0.68, 0.82, 0.91 s, etc.

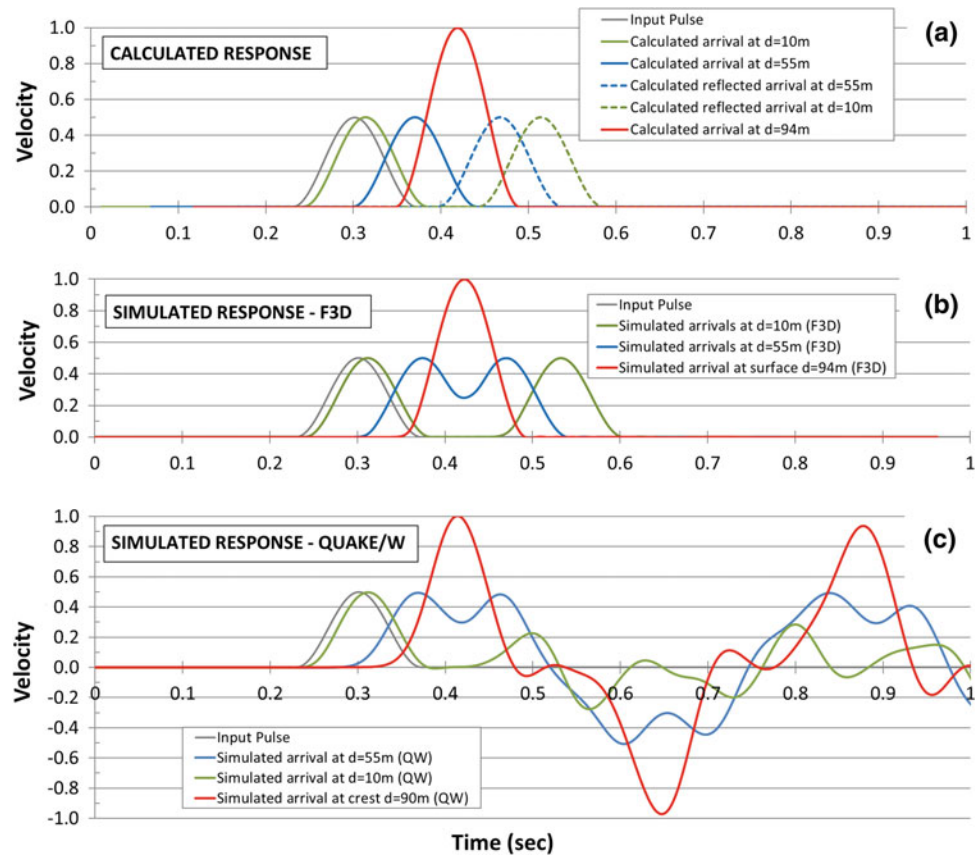
### Verification Test 2 Arrival Time of Reflected Pulse

The pulse travel time through a distance ( $d$ ) of 90 m and shear wave velocity ( $V_s$ ) of 800 m/s is 0.11 s. Thus the arrival time at the surface, for a peak initiating at 0.3 s, is 0.41 s. The calculated (Fig. 5a) and simulated arrival times (Quake/W and F3D, Fig. 5b, c) show good correlation with peak arrival at 0.41 s.

### Verification Test 3 Amplitude of Pulse at the Free Surface Boundary

The amplification of a pulse at the free boundary interface in an elastic medium is 2 (Grant and West 1965). This means that amplitude of the pulse at the surface should be twice that of the incident peak. The calculated response at the surface is plotted in Fig. 5a, with peak at  $t = 0.41$  s and amplitude of 1 m/s ( $0.5 \text{ m/s} \times 2$ ). The simulated response using F3D is shown in Fig. 5b, showing good agreement with the

**Fig. 5** Amplitude of incident pulse (Test 1), arrival time (Test 2), surface amplitude (Test 3), reflected amplitude (Test 4) and polarity (Test 5) of vertically propagating pulse reflecting at the surface. The pulse initiates at 0.3 s and is recorded by stations at 10 m (0.31 s) and 55 m (0.369 s) above the base. *Input* peak at 0.3 s shown for comparison. **a** Calculated peak. **b** Flac3D simulation. **c** Quake/W simulation. Note continued reflection effects after 0.55 s in Quake/W simulations



calculated results. The result obtained using Quake/W is shown in Fig. 5c, also correlating with the calculated response. However, as shown in Test 1, Quake/W continues to generate pulse reflection at the base. This effect could have implication in dynamic slope stability analysis by affecting the acceleration sampled by the trial slip surfaces.

#### Verification Test 4 Amplitude of the Reflected Pulse

The amplitude coefficient of a reflected pulse at the free boundary interface between two mediums is 1. This means that the amplitude of the reflected pulse should be equal to that of the incident peak. The calculated response for this test is shown in Fig. 5a, where the amplitude of the returning peaks at 55 m (0.481 s) and 10 m (0.513 s) above the base are equal to the amplitude of the incident peaks at the same locations, i.e., at 0.369 and 0.313 s. Figure 5b shows the results of simulations carried out using F3D, as measured by stations located 10 and 55 m above the base of the grid. These results are in good agreement with calculated

responses demonstrating that reflection, transmission and propagation laws are met. Figure 5c shows the results obtained using the Quake/W program. Here, peak reflection is partially met and after reflection at the surface the pulse seems to show modified amplitude inconsistent with calculated response

#### Verification Test 5 Polarity of Reflected Pulse

The polarity of a reflected pulse from a free boundary interface is positive. This means that peak of the reflected pulse should change phase with respect to that of the incident peak. This is shown Fig. 5a where the calculated peak amplitude of the pulse travelling towards the surface, i.e., at 0.313 s (10 m) and 0.369 s (55 m) have the same polarity (positive value) after they are reflected back from the surface, i.e., at 0.481 and 0.513 s. As above, it can be seen from Fig. 5c that there is a polarity reversal in the reflected pulse simulated by Quake/W. This has strong implication for interference with other peaks that would be present in a full seismic record time history.

### 2D Slope Response

The 2D slope profile shown in Fig. 1 used to simulate the velocity and acceleration response to an input Ricker wavelet applied at the base of the model with peak frequency of 7 Hz using three different programs (Quake/W, F3D and BI). Recording stations were located 10 m behind the crest of the 2D slope grid (ST1) and at the toe of the slope (ST2) as shown in Fig. 1. The simulated x-acceleration and x-velocity response at station ST1 are plotted in Fig. 6, and the peak amplitude values are summarised in Table 2. The simulated maximum peak x-velocity and x-acceleration recorded at the surface (ST1), at 0.41 s, vary from 1.1 to 1.4 m/s and 50 to 64 m/s<sup>2</sup>, respectively. An exact comparison of the response time histories is not intended in this study, and is not expected in these results. However, there are features that are relevant for comparison purposes because they reflect the numerical treatment of the software programs and have implication for interpretation of the

results. In particular, the increasing amplitudes of the Quake/W peaks after 0.5 s. These are spurious results, and are the consequence of constructive interference with vertically reflected pulses at the base of the slope grid, which would give incorrect maximum values.

### Stage 1: Regular 3D Slope Crest Versus 2D Section

A three dimensional mesh was generated by extending the two dimensional profile laterally. This was done to make a comparison between results obtained from a cross section simulation to the results obtained from a 3D model, of the same section. The 3D grid mesh is shown in Fig. 2. Numerically, in this case, the results from the 3D simulation should be similar to the 2D simulation. This is because, in this case, the profile represents a laterally infinite slope, and there are no lateral variations in slope morphology to modify

**Fig. 6** Results from 2D comparison of **a** x-velocity and **b** x-acceleration. Results from Quake/W (green), F3D (blue) and BI (red) simulations are for a vertical Ricker pulse input. Input pulse (grey) shown for comparison

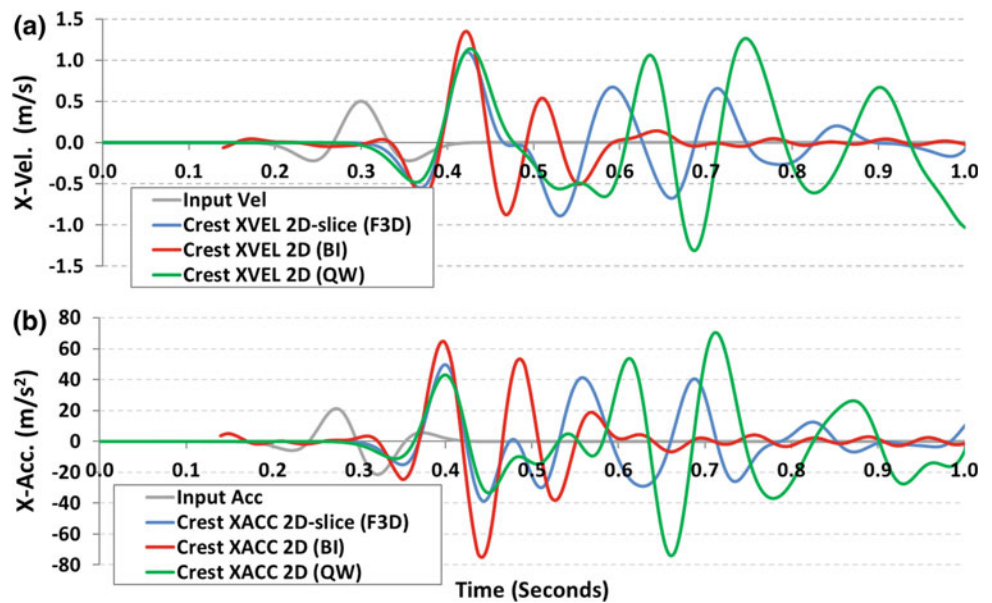
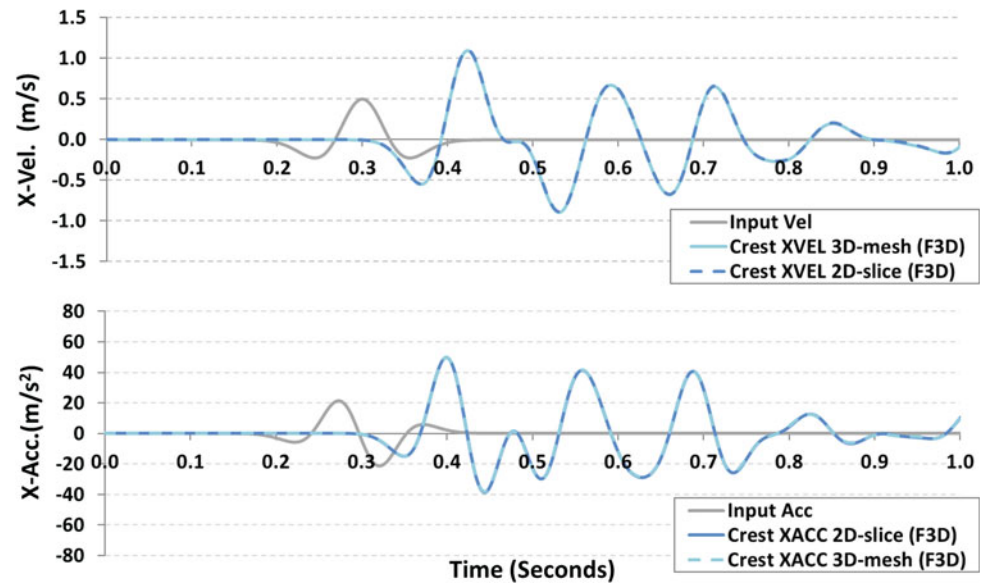


**Table 2** Simulated maximum x-velocity

Grid	2D	2D	2D	3D (Regular)	3D (Spur)
Program	F3D	Q/W	BI	F3D	F3D
X-velocity (m/s <sup>2</sup> )					
Input	0.50	0.50	0.50	0.50	0.50
Toe (ST2)	0.97	1.17	1.00	0.98	0.98
Crest (ST1)	1.10	1.26	1.35	1.10	1.27
Amplification					
Crest to toe	1.1	1.0	1.3	1.1	1.3
Crest to input	2.2	2.6	2.7	2.2	2.5
Toe to input	1.9	2.4	2.0	2.0	2.0



**Fig. 7** Comparison of results from two- and three-dimensional simulations. Input pulse shown for comparison in grey



the in-plane response. Figure 7 illustrates the simulated velocity and acceleration responses at the same crest point from 2D and 3D mesh analyses. The results are virtually identical as expected.

## Stage 2: 3D Regular Versus Irregular Slope Response

Following the above tests and verifications we determined if topographic irregularities had a contribution to the simulations otherwise obtained using a 2D analysis. The generic spur geometry in Fig. 2 was used. The response of the 3D simulations used for comparison of the results were obtained using the “regular” and “irregular” (spur) slope crest lines, using the results recorded at stations located at 5 m spacing along a 60 m long section line (in the plane of the 2D sec-

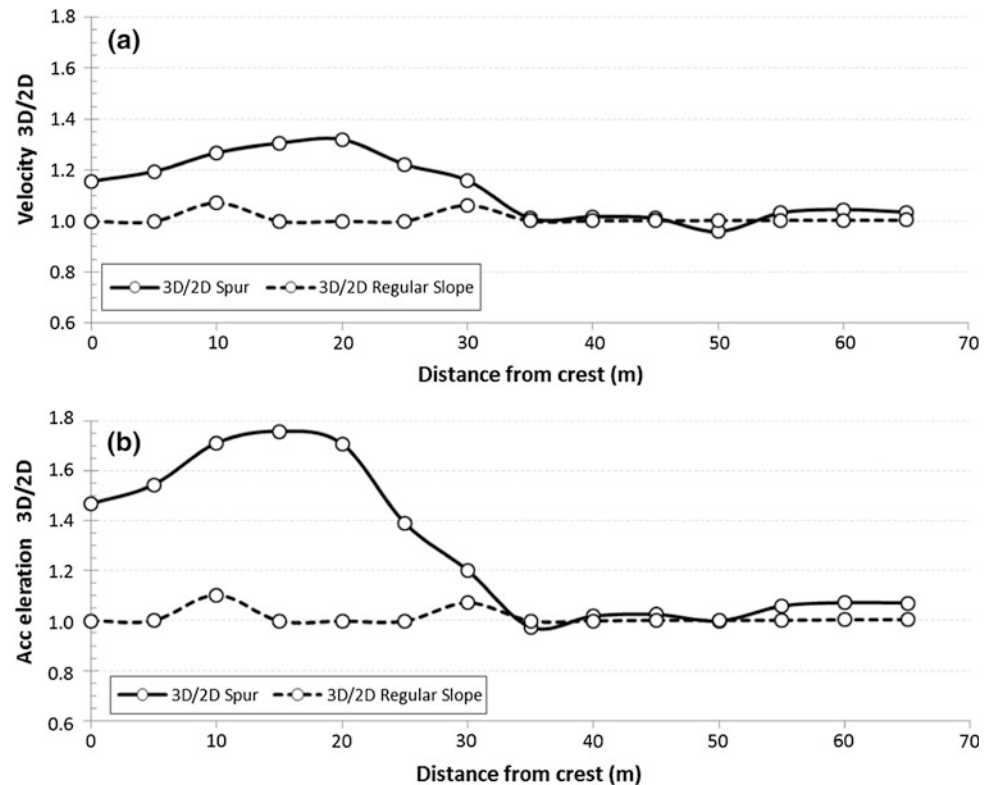
tion), as shown in Fig. 1. In this case the section line was positioned 4 m off axis to avoid cancellation effects due to grid symmetry. Results from these simulations are tabulated in Table 3. Figure 8 shows ratios of 3D/2D responses along the section line for maximum velocity (Fig. 8a) and maximum acceleration (Fig. 8b). The 3D/2D ratios computed for a regular slope crest show no significant variation (i.e., about 1). The results suggest a 2D section could be used to represent a laterally infinite and regular 3D slope geometry.

The 3D/2D ratios computed for the spur slope crest show variations of up to 1.7 as a result of the internal reflection and focusing from the spur. This means that a 2D section used to represent a complex (i.e. not laterally infinite) irregular slope could underestimate the value of maximum acceleration or maximum velocity near the crest. For this particular case study, the area of influence is about 30 m back from the slope crest (Fig. 8).

**Table 3** Simulated maximum x-acceleration

Grid	2D	2D	2D	3D (Regular)	3D (Spur)
Software	F3D	Q/W	BI	F3D	F3D
X-acceleration (m/s <sup>2</sup> )					
Input	21.0	21.3	23.7	21.0	21.0
Toe (ST2)	41.8	62.1	47.3	42.0	41.8
Crest (ST1)	49.6	69.7	64.2	49.6	65.7
X-Acc amplification					
Crest to toe	1.2	1.1	1.4	1.2	1.6
Crest to input	2.4	3.3	2.7	2.4	3.1
Toe to input	2.0	2.9	2.0	2.0	2.0

**Fig. 8** Comparison of amplification results from a “regular” and irregular “spur”. **a** is the peak velocity amplification ratio and **b** is the peak acceleration amplification ratio, between 3D and 2D results



## Conclusions

This study shows that seismic analysis based on the analysis of 2D cross sections of slopes with irregular topography such as spur crest lines could underestimate the amplification of shaking at the crest of the spur. Nonetheless, regular slope geometries representing a laterally infinite slope can be well represented by 2D analyses. The following points are noted:

1. 2D analyses require selection of carefully placed section lines. As the slope becomes more irregular, the contribution from topography needs to be given careful consideration by way of 3D simulations.
2. For flat ground surface, and adopting an elastic medium, the maximum amplitude at the ground surface ( $A_{\text{SURFACE}}$ ) should be twice that of the input motion peak ( $A_{\text{INPUT}}$ ). This means that using the input motion peak as representative of free-field peak (e.g.,  $A_{\text{FF}}$ ) is incorrect. Thus quantifying the amplification of a slope crest in terms of  $A_{\text{CREST}}/A_{\text{INPUT}}$  or is not accurate, as these ratios do not take into account the free-surface amplification effect, and these ratios will generally tend to give a value of about 2. Instead, slope amplification should be measured as crest-to-toe, to isolate this effect.

3. The quake/W software program appears to include continued internal reflection of the pulse from the base which can lead to the simulation of outputs with anomalously higher peaks than the input signal. In practice, such effects are typically dumped out, which is not technically correct.

**Acknowledgements** We thank reviewers for their constructive comments and help in preparing this manuscript. This study was funded by Strategic Development Fund (SDF) project no. 43040515-02 at the Institute of Geological and Nuclear Sciences Limited (GNS Science).

## References

- Della Pasqua F, Massey C, Lukovic B, Ries W, Archibald G (2014) Canterbury Earthquakes 2010/2011 Port Hills slope stability: earth/debris flow risk assessment for defender lane. GNS Sci Consult Rep 2014(34):132p
- Grant FS, West GF (1965) Interpretation theory in applied geophysics. McGraw-Hill, Inc., p 583
- Itasca Consulting Group (2005) Fast Lagrangian analysis of continua in 3 dimensions. Minneapolis, Itasca. Flac-3d Version 5.1
- Massey C, Taig T, Della Pasqua F, Lukovic B, Ries W, Archibald G (2014) Canterbury Earthquakes 2010/2011 Port Hills slope stability:

- debris avalanche risk assessment for Richmond Hill. GNS Sci Consult Rep 2014(34):132p
- Ricker N (1977) Transient waves in visco-elastic media. In: Developments in solid earth geophysics, vol 10. Elsevier, The Netherlands, p 278
- Massey C, Della Pasqua F (2014) Canterbury Earthquakes 2010/2011 Port Hills slope stability: debris avalanche risk assessment for Richmond Hill. GNS Sci Consult Rep 2014(34):132
- Slope/W (2012) Stability modeling with SLOPE/W. Version 8.15.5.11777. An engineering methodology fourth edition. GEO-SLOPE International Ltd
- Wong H, Jennings P (1975) Effects of canyon topography on strong earthquake motion. Bull Seis Soc Am 65:1239–1257
- Zeng Y, Benites R (1998) Seismic response of multi-layered basins with velocity gradients upon incidence of plane shear waves. Earthq Eng Struct Dyn 27:15–28